[Chem. Pharm. Bull. 28(8)2292—2300(1980)]

# Effects of the Hydrogen Bond between His 57 and Asp 102 on the Lone Pair Molecular Orbital of Nitrogen of His 57 in Serine Proteases

HIDEAKI UMEYAMA and SETSUKO NAKAGAWA

*School of Pharmaceutical Sciences, Kitasato University*[1]

(Received December 10, 1979)

The function of the hydrogen bond between His 57 and Asp 102 in serine proteases was studied by *ab initio* molecular orbital calculations on a model of the enzyme. The calculated hydrogen bond distance was 2.73 Å, which is in good agreement with the distances obtained by X-ray diffraction analyses of trypsin. The stabilization energy is −30.0 kcal/mol. The electrostatic interaction term is the dominant contributor. The polarization energy and the charge transfer energy are also significant. The charge transfer energy is largely due to charge transfer from the aspartic acid to the histidine. The lone pair molecular orbital (LPMO) level of the nitrogen of His 57 increases substantially due to the electrostatic interaction between the two molecules. As a result, the charge transfer interaction between Ser 195 and the LPMO increases, and the increase of LPMO level should play a role in lowering the barrier height of proton transfer from Ser 195 to His 57 in trypsin. The populations of the LPMO upon complex formation are changed due to the polarization term. The populations of the outer shell of the nitrogen LPMO increase substantially, and hence the stabilization energy between His 57 and Ser 195 will increase with complex formation between His 57 and Asp 102. On the basis of optimized calculations of the complex, it is suggested that the hydrogen-bond structure in trypsin involves the anion of Asp 102, the neutral form of His 57 and the neutral form of Ser 195.

**Keywords**——serine protease; trypsin; enzyme; charge relay; histidine; structure; MO; molecular orbital; quantum chemistry; *ab initio*

The reaction mechanism of serine proteases has been studied by many researchers in relation to the hydrogen bonding of Asp 102, His 57 and Ser 195, since Blow *et al.* had proposed a reaction mechanism based on a charge relay system. Hydrogen-bond structures involving a carboxyl group, imidazole group and hydroxyl group have been found in the active sites of α-chymotrypsin,[2] trypsin,[3] elastase,[4] subtilisin,[5] acyl-α-chymotrypsin,[6] lactate dehydrogenase,[7] and ribonuclease A.[8]

Two mechanisms involving hydrogen-bond structures have been proposed. One is based on a charge relay system,[2] in which two protons transfer from His 57 to Asp 102 and from Ser 195 to His 57. In this system Asp 102 lowers the barrier height of the proton transfer from

1) Location: *9-1, Shirokane 5-chome, Minato-ku, Tokyo 108, Japan.*
2) J.J. Birktoft and D.M. Blow, *J. Mol. Biol.*, **68**, 187 (1972).
3) *a*) H. Fehlhammer and W. Bode, *J. Mol. Biol.*, **98**, 683 (1975); *b*) W. Bode and P. Schwager, *ibid.*, **98**, 693 (1975); *c*) R. Huber, D. Kukla, W. Bode, P. Schwager, K. Bartels, J. Deisenhofer, and W. Steigemann, *ibid.*, **89**, 73 (1974); *d*) F.C. Bernstein, T.F. Koetzle, G.J.B. Williams, E.F. Meyer, Jr., M.D. Brice, J.R. Rodgers, O. Kennard, T. Shimanouchi, and M. Tasumi, *ibid.*, **112**, 535 (1977); *e*) R. Huber and W. Bode, *Acc. Chem. Res.*, **11**, 114 (1978).
4) L. Sawyer, D.M. Shotton, and H.C. Watson, *Biochem. Biophys. Res. Commun.*, **53**, 944 (1973).
5) *a*) J. Drenth, W.G.J. Hol, J.N. Jansonius, and R. Koekoek, *Cold Spring Harbor Symp.*, **36**, 107 (1972); *b*) R.A. Alden, J.J. Birktoft, J. Kraut, J.D. Robertus, and C.S. Wright, *Biochem. Biophys. Res. Commun.*, **45**, 337 (1971).
6) R. Henderson, *J. Mol. Biol.*, **54**, 341 (1970).
7) J.L. White, M.L. Hackert, M. Buehner, M.J. Adams, G.C. Ford, P.J. Lentz, Jr., I.E. Smiley, S.J. Steindel, and M.G. Rossmann, *J. Mol. Biol.*, **102**, 759 (1976).
8) *a*) "Atlas of Molecular Structures in Biology," Edited by D.C. Philips and F.M. Richards, 1973, p. 7; *b*) H. Umeyama, S. Nakagawa, and T. Fujii, *Chem. Pharm. Bull.*, **27**, 974 (1979).

Ser 195 to His 57, acting as a proton acceptor.[9] The other mechanism is a general base mechanism with His 57 under the influence of the anionic charge of Asp 102.[10] In this mechanism, the proton of Ser 195 transfers very easily to His 57, since the electrostatic interactions among the anion of Asp 102, the cation of His 57 and the anion of Ser 195 stabilize the structure after the proton transfer. The authors reported studies on the catalytic involvement of the hydrogen-bond structures in the active sites of serine proteases by *ab initio* calculations using a double zeta basis set.[11] The potential energy surface (Fig. 1) was described for the proton transfer from Ser 195 to His 57 ($\alpha$ transfer) and the proton transfer from His 57 to Asp 102 ($\beta$ transfer) in trypsin.[11] The results showed that Asp 102 did not accept the proton of His 57 in the enzymatic reaction, but played a significant role in lowering the barrier height of the $\alpha$ transfer.[11] In a model of trypsin, the stabilization energy between isolated His 57 and Ser 195 molecules and that between the complex of Asp 102 and His 57 and an isolated Ser 195 molecule were 9.3 and 15.0 kcal/mol, respectively.[11] The stabilization energy between the proton donor and the proton acceptor thus increased by 5.7 kcal/mol in the presence of Asp 102.[11] Therefore the change of the lone pair molecular orbital (LPMO) of $N^{\varepsilon 2}$ of an isolated His 57 molecule has a significant effect on its role as a proton acceptor. In this paper, the origin of the hydrogen bond between Asp 102 and His 57 and the origin of the effects of the hydrogen bond on the LPMO of $N^{\varepsilon 2}$ of His 57 are studied from a quantum chemical point of view.

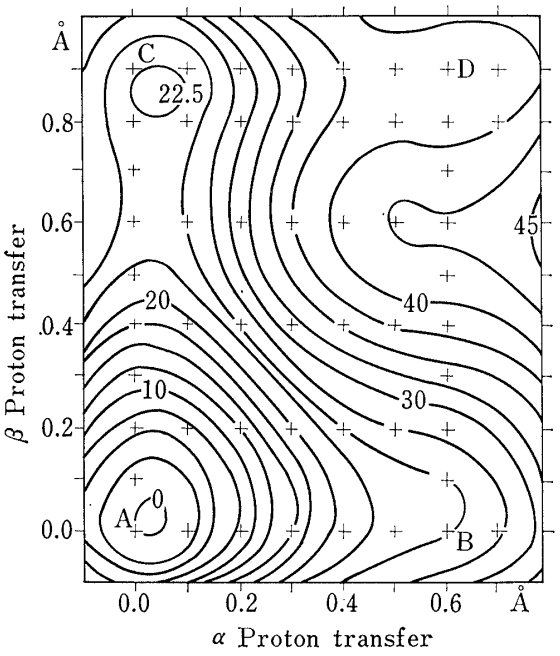


Fig. 1. The Potential Energy in kcal/mol for Proton Transfers from Ser 195 to Asp 102[11]

## Method

All the calculations were performed within the framework of a closed-shell single determinant of the *ab initio* LCAO MO SCF theory, using the Gaussian 70 program.[12] The split-valence 4-31G basis set was used with the suggested standard scale factors.[13] The details of the calculations of energy decomposition analyses and charge distribution components have been summarized in other papers.[14]

$\Delta E$ is the stabilization energy due to the complex formation, and can be divided as follows:

$$\Delta E = ES + EX + PL + CT + MIX,$$

where $ES$ is electrostatic energy, $EX$ is exchange repulsion, $PL$ is polarization energy, $CT$ is charge transfer energy, and $MIX$ is coupling energy. $EX$ can be separated into two parts, $X$ and $EX'$.

9) *a*) D.M. Blow, J.J. Birktoft, and B.S. Hartley, *Nature* (London), **221**, 337 (1969); *b*) D.M. Blow, *Acc. Chem. Res.*, **9**, 145 (1976).
10) L. Polgar and M.L. Bender, *Proc. Nat. Acad. Sci. U.S.A.*, **64**, 1335 (1969).
11) S. Nakagawa, H. Umeyama, and T. Kudo, *Chem. Pharm. Bull.*, **28**, 1342 (1980).
12) W.J. Hehre, W.A. Lathan, R. Ditchfield, M.D. Newton, and J.A. Pople, Gaussian 70, Quantum Chemistry Program Exchange, Indiana University (1974).
13) R. Ditchfield, W.J. Hehre, and J.A. Pople, *J. Chem. Phys.*, **54**, 724 (1971).
14) *a*) K. Morokuma, *J. Chem. Phys.*, **55**, 1236 (1971); *b*) K. Kitaura and K. Morokuma, *Int. J. Quantum Chem.*, **10**, 325 (1976); *c*) S. Yamabe and K.Morokuma, *J. Am. Chem. Soc.*, **97**, 4458 (1975); *d*) H. Umeyama and K. Morokuma, *ibid.*, **98**, 7208 (1976); *e*) *Idem*, *ibid.*, **99**, 1316 (1977); *f*) H. Umeyama, K. Morokuma, and S. Yamabe, *ibid.*, **99**, 330 (1977).

$$EX = X + EX',$$

where $X$ is the attractive contribution of exchange integrals, and $EX'$ is the repulsive contribution of the overlap integrals.[14] The resulting change of electron density on the atom, $\Delta\rho$, is decomposed as follows:

$$\Delta\rho = \rho_{EX} + \rho_{PL} + \rho_{CT} + \rho_{MIX},$$

where $\rho_{EX}$ is the change due to $EX$, $\rho_{PL}$ is that due to $PL$, $\rho_{CT}$ is that due to $CT$, and $\rho_{MIX}$ is that due to $MIX$.

Calculations were carried out using an M-180 computer at the Institute for Molecular Science.

**Geometries**——Imidazole and formic acid were used in place of His 57 and Asp 102 as a model of the enzyme.[15] The geometries have been described in another paper.[16] HCOOH and $HCOO^-$ were optimized from the *ab initio* calculations by using a 4-31G basis set.[16] The geometrical data for imidazole, except for the hydrogens, were based on the experimental data.[17] For $HCOO^-$, $r$(CH) is 1.1126, Å, $r$(CO) is 1.2506 Å, and ∠HCO is 114.8°.[16] For HCOOH, $r$(CH) is 1.0732 Å, $r$(CO) is 1.1960 Å, $r$(CO) is 1.3504 Å, $r$(OH) is 0.9614 Å, ∠COH is 114.6°, ∠OCO is 124.7° and ∠HCO is 110.4°.[16] For the neutral imidazole, $r$(NH) is 0.9892 Å, and $r$(CH) is 1.0622 Å.[16]

## Results and Discussion

### Electronic Structures of Isolated Molecules

The conformations of the isolated molecules of imidazole and formic acid and the total electron densities obtained from the calculations are shown in Fig. 2. The most positive position of the imidazole molecule is $H^9$, covalently bonded to the nitrogen, and the most negative position of the formic acid is $O^{10}$ (or $O^{12}$). Figure 3 shows the sigma (s) and pi (p) MO levels of the isolated molecules in hartree units. The levels from the lst MO to the 3rd MO for the formic acid and from the lst MO to the 5th MO for the imidazole are omitted, since these MO's have almost the lS character of C, O and N, respectively. The higher levels of the occupied MO's of the formic acid are closer to the zero level than those of the imidazole. Therefore, charge transfer will occur from the higher levels of the occupied MO's of the formic acid to the lower levels of the unoccupied MO's of the imidazole. In relation to the charge transfer interaction, the 10S and 11S MO's of the formic acid and the 20S MO of the imidazole will be significant, since the electron densities on the $O^{10}$, $H^9$ and $N^3$ atoms within each MO are large, as shown in Fig. 4. The electron densities within the MO are proportional to the radii of the circles in Fig. 4. Moreover, since the LPMO of $N^{\varepsilon 2}$ of His 57 in the enzymatic reaction interacts with the MO's of Ser 195, the electron densities within the LPMO of $N^1$ of the imidazole are shown in Fig. 5. The LPMO of $N^1$ corresponds to the highest occupied MO in the $\sigma$ MO's of the imidazole. The electron density, 0.443, of $2p_z$ of $N^1$ is much larger than that, 0.102, of 2s of $N^1$. The electrons are substantially localized within $2p_z$ of $N^1$ so as to react easily with a proton donor such as Ser 195.

### Complex between Imidazole and Formic Acid

In the crystal structure of bovine trypsin at 1.5 Å resolution,[3a] the distance between $O^{\delta 2}$ of Asp 102 and $N^{\delta 1}$ of His 57 and that between $O^{\delta 1}$ of Asp 102 and $N^{\delta 1}$ of His 57 are 2.75 and 3.44 Å, respectively. In the refined crystal structure of trypsin at 1.8 Å with benzamidine as an inhibitor,[3b] the above distances are 2.90 and 3.59 Å, respectively, and in the complex of bovine trypsin with bovine pancreatic inhibitor at 1.9 Å resolution[3c] these distances are 2.72 and 3.08 Å, respectively. Further, in tosyl-α-chymotrypsin they are 2.81 and 3.65 Å, respectively.[2] Since the resolutions for tosyl-elastase,[4] subtilisin (Novo)[5a] and subtilisin[5b] were 2.5, 2.8 and 2.5 Å, respectively, the relations between the histidine and the aspartic acid in the active site are not available for comparison with the calculated values in these cases. All the conformations between His 57 and Asp 102 for the serine proteases mentioned above

15) H. Umeyama, A. Imamura, C. Nagata, and M. Hanano, *J. Theoret. Biol.*, **41**, 485 (1973).
16) S. Nakagawa, H. Umeyama, K. Kitaura, and K. Morokuma, 3rd International Congress of Quantum Chemistry in Japan, 2-p-9 (1979).
17) L.E. Sutton and B. Phil, "Interatomic Distances," published by the Chemical Society, London, 1958.

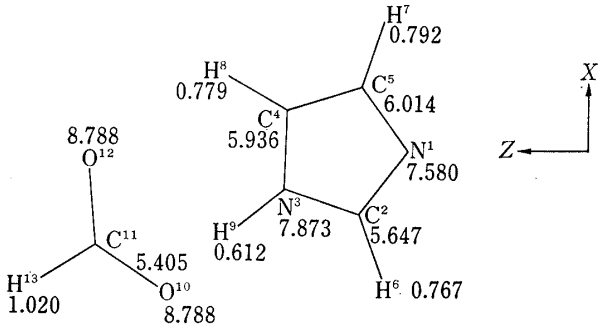


Fig. 2. Structures and the Total Electron Densities of Isolated Formic Acid and Imidazole

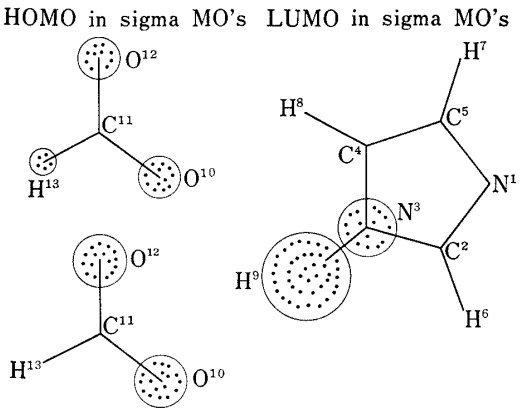


Fig. 4. Electron Densities of Atoms in the 10S, 11S, and 20S MO's of Isolated Formic acid and Imidazole

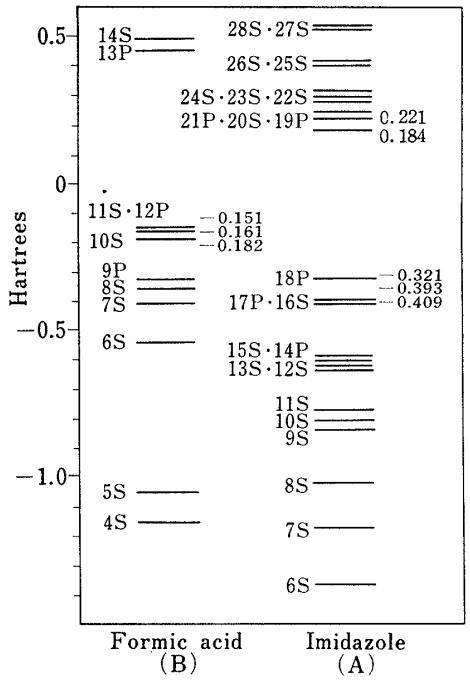


Fig. 3. MO levels of Isolated Formic Acid and Imidazole in Hartree Units

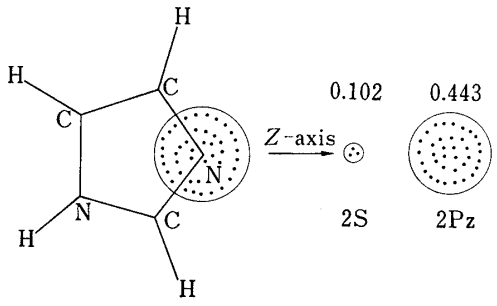


Fig. 5. Electron Density of $N^1$ in HOMO (LPMO) $\sigma$ MO's of Imidazole

involve linear hydrogen bonds between $O^{\delta 2}$ of Asp 102 and $N^{\delta 1}$ of His 57. The *ab initio* calculations of the conformations using a STO-3G basis set[18] were in good agreement with the results of X-ray diffraction analyses.[2,3] Since the results of the *ab initio* calculations suggested the linear hydrogen bond structure rather than the bifurcated hydrogen bond one,[18] optimization of the conformation within the linear hydrogen bond structure was performed using a 4-31G basis set. Figure 6 shows the optimized structure and the total electron densities at the atoms of the complex. For the complex, $r$(ON) forming the hydrogen bond and the other $r$(ON) were calculated to be 2.73 and 3.36 Å, respectively, in very good agreement with the results of the X-ray diffraction analyses as shown in Table I. The stabilization energy between the imidazole and the formic acid was calculated to be −30.0 kcal/mol. In order to elucidate the cause of the complex formation, the stabilization energy was decomposed into five terms as shown in Table II. *ES* contributes dominantly to the stabilization of the complex. *PL* and *CT* are less significant, and *MIX* is very small. Since the four terms other than *ES* depend upon the MO overlaps between the imidazole and the formic acid, EX giving the repulsive

18) H. Umeyama and S. Nakagawa, *Chem. Pharm. Bull.*, **27**, 1524 (1979).

Table I. Hydrogen Bond Distances in Å between Asp-102 and His-57 in the Active Sites of Serine Proteases, and Optimized Distances between Formic Acid and Imidazole

| | Theoretical value | Trypsin | Trypsin with benzamidine | Trypsin with BPTI | Tosyl-α-chymotrypsin |
|---|---|---|---|---|---|
| Resolution | | 1.5Å[3a] | 1.8Å[3b] | 1.9Å[3c] | 2.0Å[2] |
| $r(O^{\delta 2}N^{\delta 1})$ | 2.73 | 2.75 | 2.90 | 2.72 | 2.81 |
| $r(O^{\delta 1}N^{\delta 1})$ | 3.36 | 3.44 | 3.59 | 3.08 | 3.65 |

Table II. Stabilization Energy in kcal/mol and Energy Decomposition Analysis between Imidazole (A) and Formic Acid (B) using a 4-31G Basis Set

| Term | Energy |
|---|---|
| $\Delta E$ | −30.0 |
| $ES$ | −30.2 (67%) |
| $EX$ | 14.6 |
| $PL$ | −6.1 (14%) |
| $CT$ | −5.9 (13%) |
| $MIX$[a] | −2.8 (6%) |
| $CT_{B\to A}$[b] | −5.3 (88%)[c] |
| $EX'$[d] | 30.6 |
| $X$[d] | −16.1 |

a) $\Delta E = ES + EX + PL + CT + MIX$
b) Charge transfer from formic acid to imidazole.
c) Rate is obtained from $CT_{B\to A}/CT \times 100$.
d) $EX = EX' + X$

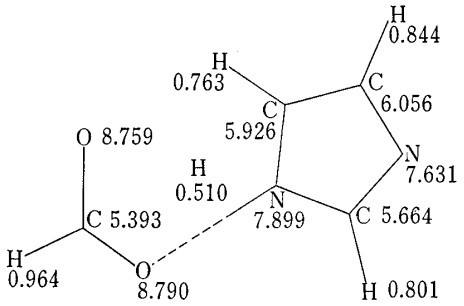


Fig. 6. Optimized Structure of the Complex between Formic Acid and Imidazole and Total Electron Densities of Atoms

∠CO···N=108.6°
$r$(O···N)=2.73 Å
$r$(NH)=0.9892 Å

energy can be compared with $PL+CT+MIX$ giving the attractive energy. The absolute value of $EX$ is comparable with that of $PL+CT+MIX$, and hence the repulsive energy is balanced by the attractive energy as regards MO overlaps. The charge transfer energy is almost entirely due to $CT$ from the formic acid to the imidazole, as shown in Table II. The value of the attractive contribution of exchange integrals is 16.1 kcal/mol, and the value of the repulsive contribution is 30.6 kcal/mol. Figure 7 shows the MO levels of the isolated imidazole and the complexed imidazole. The levels of $\sigma$ MO's of the imidazole increase substantially on complex formation. The MO levels obtained from the SCF calculations including only the electrostatic interaction are very similar to those of the complex. Therefore the increase of the MO levels in the complex formation is due to $ES$. The $\pi$ MO levels and the $\sigma$ MO levels change similarly, as shown in Fig. 8. Since the formic acid interacts with the imidazole through the hydrogen bond, the $\sigma$ MO's of the imidazole are thought to be considerably affected by the $\sigma$–$\sigma$ interactions of the two molecules. However, the $\pi$ MO's of the imidazole are also considerably affected by the interactions. This similarity of the changes of the $\sigma$ and $\pi$ MO's presumably arises from the large contribution of $ES$.

## Total Electron Density Changes due to Complex Formation

The total electron densities of the atoms change due to interactions during complex formation. Table III shows these changes and the results of energy decomposition analysis (see also Fig. 9). The dotted and open circles in Fig. 9 represent electron increase and electron decrease, respectively; the radii of the circles are in proportion to the total electron density changes. The total electron density changes of $O^{10}$, $H^9$ and $N^3$ are interesting in relation to the change of the electronic structure in the formation of the hydrogen bond. The total

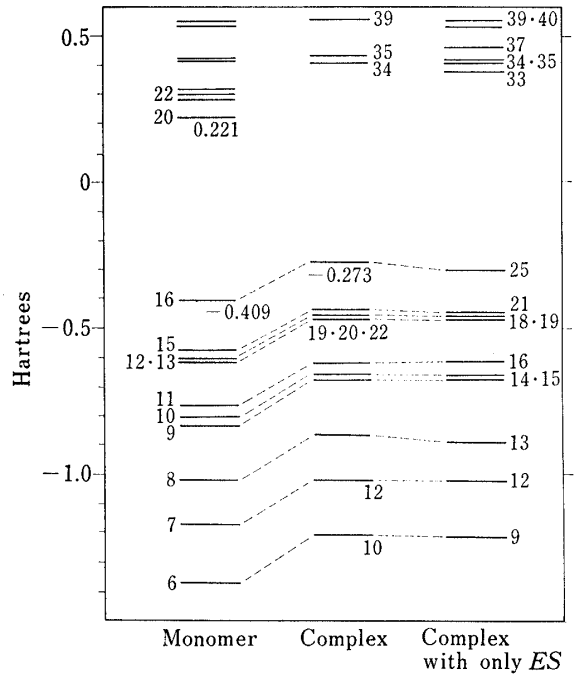


Fig. 7. Changes of $\sigma$ MO's of Imidazole on Complex Formation between Formic Acid and Imidazole

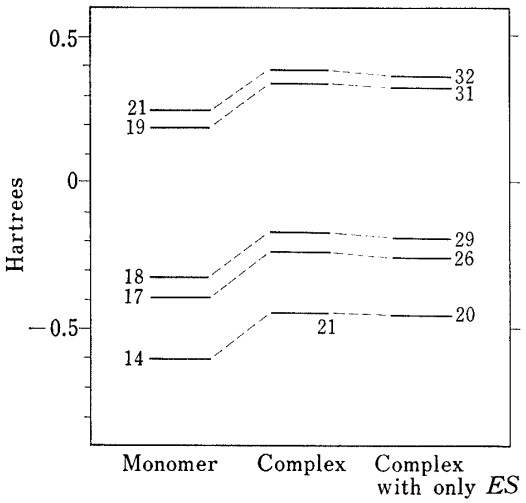


Fig. 8. Changes of $\pi$ MO's of Imidazole on Complex Formation between Formic Acid and Imidazole

electron density of $O^{10}$ of the formic acid does not change, while that of $H^9$ of the imidazole decreases substantially, and that of $N^3$ of the imidazole increases. The increase of the total electron density of $O^{10}$ due to *PL* is almost canceled out by the decreases due to *CT*+*MIX*. The decrease of the total electron density of $H^9$ is almost entirely due to *PL*, since the increasing effect due to *CT* cancels out the decreasing effect due to *MIX*. The increase of the total electron density of $N^3$ is due to *MIX*, since the increased value due to *MIX* is larger than the decreased value due to *PL*. The large increase and the decrease of the total electron densities at $C^5$ and $C^4$, respectively, are due to *PL*. Due to *CT*, electron transfer occurs from $O^{10}$ of the formic acid to $H^9$ of the imidazole. Due to *MIX*, electron transfer occurs from $O^{10}$ of the formic acid and $H^9$ of the imidazole to $N^3$ of the imidazole. Due to *PL*, the electron density of $O^{10}$ increases, and those of $H^9$ and $N^3$ of the imidazole decrease. The decreases of the total electron densities of $H^{13}$, $C^{11}$ and $O^{12}$ of the formic acid are due to *PL*. The increases

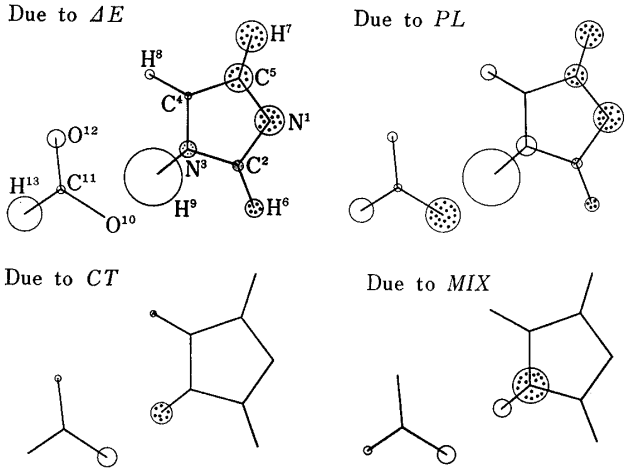


Fig. 9. Total Electron Density Changes due to the Terms $\Delta E$, *PL*, *CT*, and *MIX*

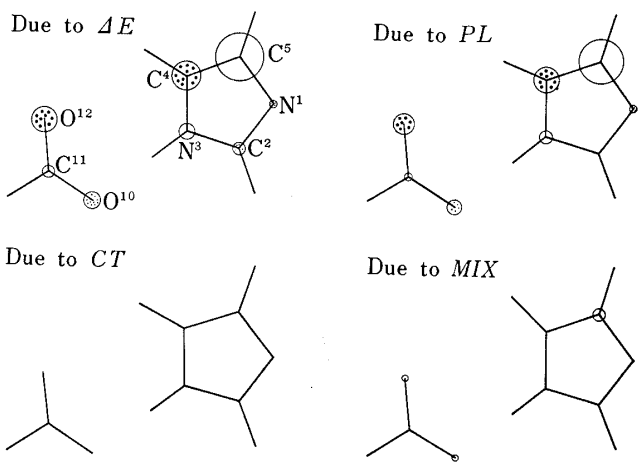


Fig. 10. $\pi$ Electron Density Changes due to the Terms $\Delta E$, *PL*, *CT*, and *MIX*

in the total electron densities of $N^1$, $C^2$, $C^5$, $H^6$ and $H^7$ of the imidazole are also due to *PL*. Figure 10 shows the $\pi$ electron density changes of the atoms. These changes are due to *PL*. The $\pi$ electron densities of $O^{12}$ and $O^{10}$ of the formic acid increase. For the imidazole, the $\pi$ electron densities at $C^4$ and $C^5$ increase and decrease, respectively. Figure 11 shows the $\sigma$ electron density changes of the atoms. Figure 11 is similar to Fig. 9 except for the total electron densities of $O^{12}$, $O^{10}$, $C^4$, and $C^5$. Therefore the $\sigma$ electron density changes contribute dominantly to the total electron density changes.

**Change of LPMO of Imidazole on Complex Formation**

In trypsin, the complex composed of Asp 102 and His 57 interacts with Ser 195 more strongly than His 57 interacts with Ser 195 by 5.7 kcal/mol.[11] The change of the LPMO in the interaction between Asp 102 and His 57 causes an increase of the interaction energy between His 57 and Ser 195. The squared value of the MO coefficient of $N^1_{2p_z}$ AO in the isolated imidazole is almost the same as the value, 0.442, for the complex. Therefore the higher the LPMO level, the larger the charge transfer energy between the LPMO of the imidazole and Ser 195 becomes. The change of the LPMO on complex formation can be decomposed into several components as shown in Fig. 12. The energy levels are plotted relative to the LPMO in the complex. The LPMO on complex formation increases by 86 kcal/mol. About

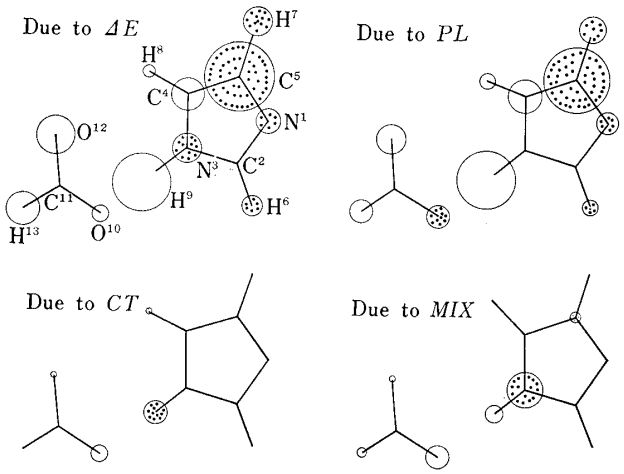


Fig. 11. $\sigma$ Electron Density Changes due to the Terms $\Delta E$, *PL*, *CT*, and *MIX*

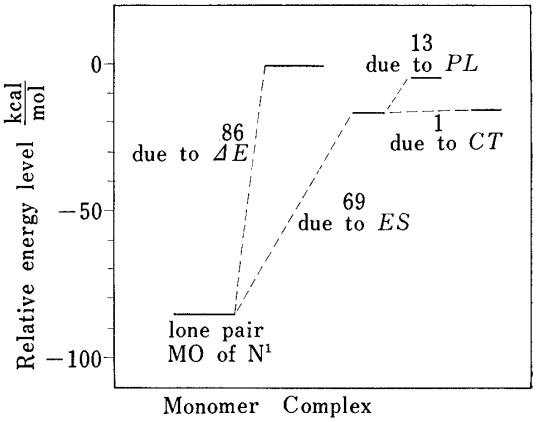


Fig. 12. LPMO Change of $N^1$ due to the Complex Formation between Formic Acid and Imidazole, and Analyses of the LPMO Change

Table III. Total Electron Density Changes due to the Stabilization Energy, and the Energy Decomponents

| Atom | $\Delta\rho_{\Delta E}$ | $\Delta\rho_{EX}$ | $\Delta\rho_{PL}$ | $\Delta\rho_{CT}$ | $\Delta\rho_{MIX}$ |
|---|---|---|---|---|---|
| $N^1$ | 0.051 | 0.001 | 0.048 | 0.001 | 0.001 |
| $C^2$ | 0.017 | 0.000 | 0.015 | 0.001 | 0.001 |
| $N^3$ | 0.026 | 0.008 | −0.037 | −0.003 | 0.058 |
| $C^4$ | −0.010 | 0.001 | −0.011 | 0.002 | −0.002 |
| $C^5$ | 0.042 | 0.000 | 0.039 | 0.000 | 0.003 |
| $H^6$ | 0.034 | 0.000 | 0.027 | 0.000 | 0.007 |
| $H^7$ | 0.052 | 0.000 | 0.047 | 0.000 | 0.005 |
| $H^8$ | −0.016 | −0.001 | −0.028 | 0.010 | 0.003 |
| $H^9$ | −0.102 | −0.010 | −0.100 | 0.038 | −0.030 |
| $O^{10}$ | 0.002 | 0.000 | 0.062 | −0.032 | −0.028 |
| $C^{11}$ | −0.012 | −0.001 | −0.009 | −0.003 | 0.001 |
| $O^{12}$ | −0.029 | 0.000 | −0.015 | −0.011 | −0.003 |
| $H^{13}$ | −0.056 | 0.000 | −0.039 | −0.004 | −0.013 |

Table IV. Electron Density Change of $N^1$ due to the Interaction between Imidazole and Formic Acid, and the Decomposition Terms

| AO | | $\rho^{a)}$ | $\Delta\rho_{AE}{}^{b)}$ | $\Delta\rho_{PL}{}^{c)}$ |
|---|---|---|---|---|
| 1S | | 1.997 | 0.000 | 0.000 |
| 2S | | 1.816 | −0.022 | −0.019 |
| | $2S_i{}^{d)}$ | 0.706 | −0.008 | −0.007 |
| | $2S_o{}^{e)}$ | 1.110 | −0.014 | −0.012 |
| $2P_x$ | | 0.958 | 0.009 | 0.009 |
| | $2P_{x_i}$ | 0.688 | 0.001 | 0.001 |
| | $2P_{x_o}$ | 0.270 | 0.009 | 0.008 |
| $2P_y$ | | 1.215 | 0.035 | 0.034 |
| | $2P_{y_i}$ | 0.615 | 0.011 | 0.011 |
| | $2P_{y_o}$ | 0.600 | 0.024 | 0.023 |
| $2P_z$ | | 1.595 | 0.027 | 0.023 |
| | $2P_{z_i}$ | 0.929 | −0.003 | −0.004 |
| | $2P_{z_o}$ | 0.665 | 0.031 | 0.028 |

*a*) AO electron densities of $N^1$ of the isolated imidazole.
*b*) AO electron density change due to the interaction between imidazole and formic acid.
*c*) AO electron density change due to the polarization interaction.
*d*) "i" shows the inner part of the 2S AO.
*e*) "o" shows the outer part of the 2S AO.

80% is due to the *ES* term, and about 15% is due to the *PL* term. The *CT* term does not contribute to the change of the LPMO.

The total electron density of $N^1$ of the imidazole is composed of the atomic orbital (AO) densities. The AO densities of $N^1$ of the isolated imidazole and the change on complex formation between the imidazole and the formic acid are shown in Table IV. The AO density changes on complex formation are largely due to *PL* as shown in Table IV. On complex formation, the value of 2s AO density decreases and those of $2p_y$ and $2p_z$ increase. The increase of that of $2p_z$ is due to the outer part AO which overlaps substantially with the hydrogen of Ser 195. Therefore the increase of the interaction between His 57 and Ser 195 arises from the change of the $2p_z$ outer electron density.

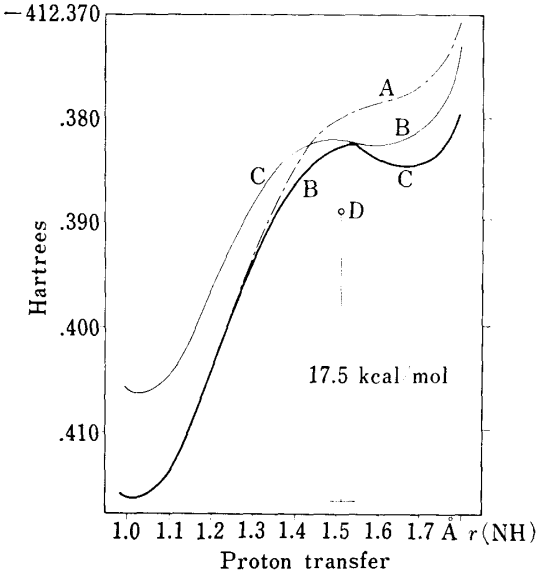


Fig. 13. Various Potential Energy Curves of Proton Transfer between Formic Acid and Imidazole, and of that between Formate and Anion Imidazole

A; $r$(ON) is 2.73 Å, $r$(CO) is 1.25 Å, and ∠CON is 109.6°.
B; $r$(ON) is 2.73 Å, $r$(CO) is 1.25 Å, and ∠CON is optimized for proton transfer.
C; $r$(CO) is 2.73 Å, (CO) is 1.35 Å, and ∠CON is optimized for proton transfer.
D; $r$(CO) is 2.60 Å, $r$(ON) is 1.35 Å, ∠CON is 114.6°, and $r$(OH) is 1.08 Å.

## Potential Energy Curves of the Proton Transfer from Imidazole to Formic Acid

The potential energy surface of the two proton transfers from Ser 195 to His 57 and from His 57 to Asp 102 in the active site of trypsin showed that the proton of His 57 does not transfer from His 57 to Asp 102 in the enzymatic reaction.[11] The barrier height of proton transfer from His 57 to Asp 102 in the active site model of Asp 102, His 57 and Ser 195 is similar to that in the complex between Asp 102 and His 57.[11] Therefore, the conclusions obtained in the study of the complex between Asp 102 and His 57 should be helpful in deciding the mechanism of the enzymatic reaction. The potential energy curves of the proton transfer are shown

for various conformations between the imidazole and the formic acid in Fig. 13. Curve A shows that the proton of the imidazole transfers in the optimized structure from neutral imidazole to the formic acid. Curve B shows the proton transfer, the CON angle being optimized for the A curve. Curve C shows the proton transfer in a structure composed of the formate and the anionic imidazole, the CON angle being optimized for the A curve. At 2.73 Å optimized distance between the formic acid and the neutral imidazole, the lowest potential curve is shown by a thick solid line. The point D shows the structure after proton transfer, in which the complex structure is optimized. The barrier height of proton transfer from the imidazole to the formic acid is estimated to be 17.5 kcal/mol. Accordingly, the proton covalently bonded to $N^{\delta 1}$ of His 57 will not transfer to $O^{\delta 2}$ of Asp 102 in trypsin.